



Defective mesoporous $\text{Li}_4\text{Ti}_5\text{O}_{12-y}$: An advanced anode material with anomalous capacity and cycling stability at a high rate of 20 C

Xiaomei Chen^a, Xiangfeng Guan^b, Liping Li^a, Guangshe Li^{a,*}

^a State Key Lab of Structural Chemistry, Fujian Institute of Research on the Structure of Matter, Chinese Academy of Sciences, Fuzhou 350002, People's Republic of China

^b Key Lab of Coal to Ethylene Glycol and Its Related Technology, Fujian Institute of Research on the Structure of Matter, Chinese Academy of Sciences, Fuzhou 350002, People's Republic of China

ARTICLE INFO

Article history:

Received 19 December 2011

Received in revised form 5 March 2012

Accepted 7 March 2012

Available online 3 April 2012

Keywords:

Lithium-ion batteries

Lithium titanate

Defective

Mesoporous

ABSTRACT

How to obtain an excellent capacity and cycling stability of electrodes that work at high rates is now challenging the development of lithium-ion batteries. Herein, we initiate a facile solvothermal method to prepare defective mesoporous $\text{Li}_4\text{Ti}_5\text{O}_{12-y}$ as an anode material with an improved high-rate performance for lithium-ion batteries. The high-rate performance for the resultant anode is represented by a discharge capacity of 139 mAh g^{-1} at a high rate of 20 C with a capacity retention of 91.4% over 300 cycles. Different from the strategies popularly used in literature, the current approach does not rely on any aids from conductive layers or foreign dopants, but takes advantages of the unique features of a defective mesoporous structure with oxygen vacancies and $\text{Ti}^{3+}-\text{O}^{2-}-\text{Ti}^{4+}$ pairs. These features enable an improved intrinsic electronic conductivity, which leads to a high-rate performance and cycling stability superior to the stoichiometric mesoporous counterpart when annealing in air. The defective mesoporous $\text{Li}_4\text{Ti}_5\text{O}_{12-y}$ is therefore demonstrated to be a promising advanced anode material for high-rate lithium-ion batteries.

© 2012 Elsevier B.V. All rights reserved.

1. Introduction

Lithium-ion batteries have drawn considerable attention for their broad class of important applications due to the high energy density, low cost, and high-rate capability [1,2]. For some practical applications like hybrid electric vehicles or electric vehicles, lithium ion batteries have to be re-charged very fast, and therefore the relevant electrode materials have to work at high rates, while maintaining the excellent capacity and cycling stability. Among all electrode materials, spinel $\text{Li}_4\text{Ti}_5\text{O}_{12}$ is a promising anode material for its good cycling stability, which is due to zero-strain properties during lithium ion insertion and extraction processes, and its relatively high potential at 1.55 V, which can effectively suppress the formation of solid-electrolyte interfaces, and thus providing an improved safety for lithium-ion batteries [3–5]. However, it is still very difficult to retain a high capacity and cycling stability at high rates, because electronic conductivity for $\text{Li}_4\text{Ti}_5\text{O}_{12}$ is usually very low, $<10^{-13} \text{ S cm}^{-1}$ [6]. To improve the rate capability of $\text{Li}_4\text{Ti}_5\text{O}_{12}$, many efforts have been done, which include (i) preparation of small-sized $\text{Li}_4\text{Ti}_5\text{O}_{12}$ with various morphologies [7,8]; (ii) coating carbon or other conductive agents on the surface of $\text{Li}_4\text{Ti}_5\text{O}_{12}$ [3]; and (iii) doping foreign metal ions (e.g., V^{5+} [9], Sr^{2+} [10], Al^{3+} [11])

into the lattice of $\text{Li}_4\text{Ti}_5\text{O}_{12}$. All these suffer from the difficulties in rational handling due to the complicated procedures, and are thus not in favor of practical applications. It appears very important to explore some simple methods for $\text{Li}_4\text{Ti}_5\text{O}_{12}$ to work at high rates.

We assumed that defective mesoporous $\text{Li}_4\text{Ti}_5\text{O}_{12-y}$ could be an ideal electrode material at high rates, based on the following 3-fold considerations: (i) $\text{Li}_4\text{Ti}_5\text{O}_{12}$ has merits of cycling stability and safety; (ii) $\text{Li}_4\text{Ti}_5\text{O}_{12}$, when prepared in a defective structure, has abundant oxygen vacancies and $\text{Ti}^{3+}-\text{O}-\text{Ti}^{4+}$ pairs, which can effectively enhance the electronic conductivity [12–15]; and (iii) $\text{Li}_4\text{Ti}_5\text{O}_{12}$, when prepared in a mesoporous structure, will have the shortened electron or lithium-ion transport pathways, which can decrease the polarization and further enhance the electrochemical performance at high rates [3,16]. Unfortunately, defective mesoporous $\text{Li}_4\text{Ti}_5\text{O}_{12-y}$ has not been reported till now, and thus it is not clear whether defective mesoporous $\text{Li}_4\text{Ti}_5\text{O}_{12-y}$ can work at high rates as promising as it does at low-rates.

In this work, we successfully prepared defective mesoporous $\text{Li}_4\text{Ti}_5\text{O}_{12-y}$ by initiating a facile solvothermal method with a subsequent N_2 treatment. Using this method, Ti^{3+} is first introduced into the mesoporous $\text{Li}_4\text{Ti}_5\text{O}_{12}$ to generate a defective structure with oxygen vacancies, which has led to an apparent increase in intrinsic electronic conductivity and furthermore an enhanced electrochemical performance. The resultant defective mesoporous $\text{Li}_4\text{Ti}_5\text{O}_{12-y}$ is found to work pretty well at a high rate of 20 C. The method reported here is novel, which does not need any aids from the

* Corresponding author. Tel.: +86 591 83702122; fax: +86 591 83702122.

E-mail address: guangshe@fjirsm.ac.cn (G. Li).

conductive layers or foreign dopants popularly used in previous literatures.

2. Experimental

Defective mesoporous $\text{Li}_4\text{Ti}_5\text{O}_{12-y}$ was prepared by developing a solvothermal method with a subsequent annealing in N_2 . In a typical process, a suspension of 1.2 g glycine and 60 mL anhydrous ethanol was stirred for 1 h. A relatively stable suspension was then obtained by removing off the large glycine particles, and then 3 mL titanium *n*-butoxide ($\text{Ti}(\text{OBu})_4$) and 0.296 g lithium hydroxide monohydrate ($\text{LiOH}\cdot\text{H}_2\text{O}$) were added slowly into the suspension, which was stirred for 3 h. The suspension was then transferred into a 100 mL autoclave and maintained at 200°C for 20 h. The product was collected by filtration and washed with anhydrous ethanol for several times and dried at 80°C . The sample was finally obtained by annealing the product in N_2 at 500°C for 2 h, which gives the defective mesoporous sample: LTO-N. For comparison, a parallel sample preparation was done: stoichiometric mesoporous sample, LTO-A was synthesized under the similar conditions but treated in air.

Crystal structures of the samples were examined by X-ray diffraction (XRD) using a Rigaku MinFlex II benchtop X-ray diffractometer with a copper target. The lattice parameters were calculated by a least-squares method. Morphology and crystalline structure of the samples were observed by field-emission scanning electron microscopy (FE-SEM, JEOL JSM-6700) and high-resolution transmission electron microscopy (HR-TEM, JEOL JEM-2010). Nitrogen adsorption-desorption isotherms were measured on Micromeritics ASAP 2000 surface area and porosity analyzer. The pore size distribution and specific surface area of the sample were derived using the Barrett-Joyner-Halenda (BJH) model and the multipoint Braunauer-Emmett-Teller (BET) method, respectively. Electron paramagnetic resonance (EPR) spectra were recorded on a Bruker ELEXSYS E300 spectrometer at room temperature (X-band frequency, microwave power of 5.04 mW, and 9.86 GHz field modulation).

Total electrical conductivities of the samples were measured using alternating current impedance spectroscopy on an impedance analyzer (Agilent 4294A) in the frequency range of 40 Hz to 5 MHz at room temperature with an oscillation voltage of 0.5 V. The impedance data were analyzed by an equivalent circuit model using the Zsimpwin program. The electronic conductivities were determined using direct current measurement on a digital source meter (Keithley 2400). For all measurements, samples of given mounts were pressed uni-axially into pellets with a diameter of 7 mm and about 2 mm in thickness. Silver paste was painted onto both sides of pellets as electrodes. All pellets were tightly compressed at room temperature without sintering.

Electrochemical performance of the samples was characterized using CR2025 coin-type cells. The electrodes were fabricated by mixing the as-prepared $\text{Li}_4\text{Ti}_5\text{O}_{12-y}$ powders, acetylene black, and poly(vinylidene fluoride) at weight ratios of 70:15:15, respectively, using *N*-methyl pyrrolidone as a solvent. The slurry was then casted onto copper foil current collector and dried at 100°C in vacuum. After the evaporation of the solvent, disks of 1.54 cm^2 were punched out of the foil. For comparison, the loadings of the samples on each disk were set at a similar level about 1.3 mg cm^{-2} . The cells were assembled in an Ar-filled glovebox by using lithium foil as the counter electrode and a polypropylene film as the separator. The electrolytes were 1 M LiPF_6 dissolved in ethyl carbonate (EC), diethyl carbonate (DEC) and dimethyl carbonate (DMC) in a volume ratio of 1:1:1. The cells were charged and discharged galvanostatically using a battery tester (Land Battery Test System) in a voltage range of 3.0–1.0 V (vs. Li^+/Li) at room temperature. Cyclic voltammetry were carried out on an electrochemical workstation

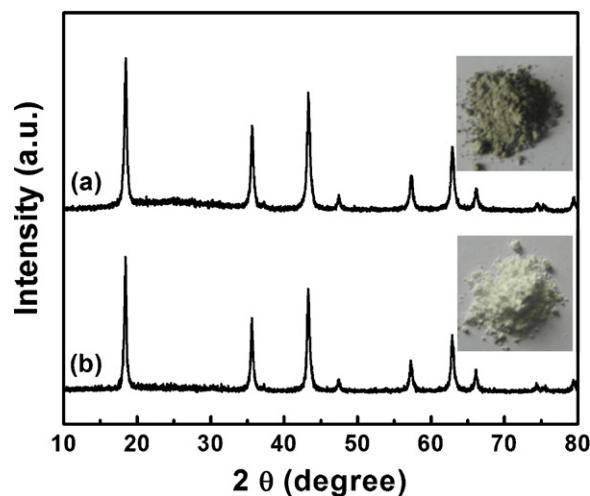


Fig. 1. XRD patterns of the samples: (a) LTO-N and (b) LTO-A. Insets show the corresponding sample colors.

(CHI660 C) between 3.0 V and 1.0 V at sweep rates varied from 0.6 to 1 mV s^{-1} .

To study the conductivity effect on cycle rates, 5 wt% carbon was mixed with the as-prepared LTO-N and LTO-A powders before electrode preparation, while other experimental conditions were maintained. The resultant samples of carbon mixed with LTO-N and LTO-A were named as LTO-N-C and LTO-A-C, respectively.

3. Results and discussion

Fig. 1 shows XRD patterns of the LTO-N and LTO-A samples. It is observed that all XRD peaks for the two samples are sharp, which indicates high crystallinity. Further, all these diffraction peaks are well indexed to a cubic spinel structure of $\text{Li}_4\text{Ti}_5\text{O}_{12}$ (space group: $\text{Fd}\bar{3}m$, JCPDS, No. 49-0207), while no other impurity phases are observed. Therefore, single-phase $\text{Li}_4\text{Ti}_5\text{O}_{12}$ with a high crystallinity is obtained for LTO-N and LTO-A. The chemical compositions for the samples were also analyzed by elemental analyzer. It is found that the residual carbon amount in LTO-N and LTO-A are as low as 0.76% and 0.66%, respectively. In spite of single phases and similar chemical compositions, the samples' colors are quite different: For LTO-N, the sample color is gray, which compared to the white color for LTO-A. It seems that Ti^{3+} and the relevant defects are present in LTO-N, as already indicated in a previous literature [15].

Morphologies and particle sizes for samples were examined by SEM and HRTEM. As indicated in Fig. 2a, sample LTO-N consists of submicron-size secondary quasi-spheres (100–500 nm) as accumulated by nanosized primary particles. These primary particles are further observed to have a dimension about 15–25 nm from the HRTEM images (Fig. 2b). The *d*-spacing for plane (111) is 0.48 nm, in good accordance with that previously reported for spinel $\text{Li}_4\text{Ti}_5\text{O}_{12}$ [17]. Further, as indicated by SEM and TEM images (Fig. 2c and 2d), LTO-A shows morphology and particle sizes quite similar to those of LTO-N. Namely, both samples were aggregates formed by nanosized primary particles with dimension of about 15–22 nm. The electron-diffraction patterns for LTO-N and LTO-A exhibit sharp spots (not shown). Therefore, both samples are demonstrated to have a high crystallinity.

Pore size distribution and BET surface area for samples LTO-N and LTO-A were investigated by N_2 adsorption/desorption analysis. From the pore size distribution curve in Fig. 3a, the average pore size for LTO-N is determined to be 3.6 nm, which is likely resulted from

Download English Version:

<https://daneshyari.com/en/article/7743621>

Download Persian Version:

<https://daneshyari.com/article/7743621>

[Daneshyari.com](https://daneshyari.com)